Journal of Geodesy manuscript No.
(will be inserted by the editor)

Systematic error mitigation in multi-GNSS positioning based on semiparametric estimation

Wenkun Yu · Xiaoli Ding · Wujiao Dai · Wu Chen

Received: date / Accepted: date

Abstract Joint use of observations from multiple Global Navigation Satellite Systems (GNSS) is advantageous in high accuracy positioning. However, systematic errors in the observations can significantly impact on the positioning accuracy if such errors cannot be properly mitigated. The errors can distort least squares estimations and also affect the results of variance component estimation that is frequently used to determine the stochastic model when observations from multiple GNSS are used. We present an approach that is based on the concept of semiparametric estimation for mitigating the effects of the systematic errors. Experimental results based on both simulated and real GNSS datasets show that the approach is effective, especially when applied before carrying out variance component estimation.

Keywords Multi-GNSS positioning · Systematic errors · Semiparametric estimation · Variance component estimation

1 Introduction

Integration of data from multiple GNSS (Global Navigation Satellite Systems, including GPS, Beidou, GLONASS and Galileo) offers great advantages, such as more visible satellites, enhanced system integrity and better geometric strength (Hofmann-Wellenhof et al, 2008; Yang et al, 2011; Leick et al, 2015). Much research efforts have been put into the various problems involved in positioning based on data from multiple GNSS (e.g., Wang et al, 2001; Shi et al, 2013; Teunissen et al, 2014; Li et al, 2015), including refining weighting schemes considering the heteroscedastic data qualities of the different satellite systems (e.g., Wang et al, 2001; Cai et al, 2014). However, relatively less attention has been given in such system integration to impacts of systematic errors that can come from, e.g., unmodeled atmospheric refraction, multipath effect and hardware delay (e.g., Schüler, 2005; Hoque and Jakowski, 2007; Wanninger, 2012; Dong et al, 2016). In addition, inter-system differences may exist. For instance, Beidou signals may be more susceptible to multipath effect compared to GPS due to its mixed constellation structure (Ye et al, 2014). Shi et al (2013) observed that biases in GPS-only solutions are normally smaller than those in Beidou-only solutions, and in some cases, solutions based on data from multiple GNSS are even more biased than solutions based on data from GPS only. Compared to code division multiple access GNSS, frequency division multiple access GLONASS observations are affected more by the hardware delays that cause inter-frequency biases (Wanninger, 2012). Even for systems with overlapping frequencies, e.g., GPS and Galileo, their inter-system biases cannot be neglected when receivers of different types are involved (Paziewski and Wielgosz, 2015). Another example is the integration of pseudolite and GPS (Meng et al, 2004). It has been reported that the positioning accuracy is significantly degraded when pseudolite observations with strong multipath signals are included. The conventional parametric estimation and variance component estimation (VCE) based on least squares (LS) principle require that the observations are free from systematic errors. Therefore when systematic errors are present, the quality of the solutions will be deteriorated (e.g., Xu, 1991).

Four approaches have been employed to mitigate systematic errors in GNSS data processing,

(1) Differencing and linear combinations of observables (e.g., Hofmann-Wellenhof et al, 2008; Leick et al, 2015). The

Wenkun Yu · Xiaoli Ding (✉) · Wu Chen
Department of Land Surveying & Geo-informatics, The Hong Kong Polytechnic University, Hung Hom, Kowloon, Hong Kong, China
Tel: +852-2766-5965 Fax: +852-2330-2994
E-mail: xl.ding@polyu.edu.hk

Wujiao Dai
School of Geosciences & Info-physics, Central South University, 410083, Changsha, Hunan, China

approach cancels out the effects of common errors (e.g. clock errors), and reduces the effects of correlated or frequency sensitive errors (e.g., tropospheric and ionospheric errors);

(2) Applying corrections based on empirical models and precise products (e.g., Satirapod et al, 2003; Meng et al, 2004; Kouba, 2015; Dong et al, 2016);

(3) Parameterization in the functional model (e.g., Paziewski and Wielgosz, 2015; Tian et al, 2015). For example, when GNSS receivers of different types are involved, additional parameters can be used to estimate the biases. Penalization parameters can be added when different GNSS are not compatible (Yang et al, 2011); and

(4) Stochastic modeling (Wang et al, 2001; Schüler, 2005). Once the major parts of systematic errors have been removed, the remaining parts are modeled stochastically.

In practice, approaches (3) and (4) are often used after applying approaches (1) and (2).

The above mentioned methods all have their limitations in mitigating the systematic errors. In (1), errors such as the higher-order ionospheric effects cannot be mitigated using linear combinations of observables (Hoque and Jakowski, 2007). The differencing approach becomes ineffective in removing the orbit errors and atmospheric refraction when the baselines are long, and the multipath errors even in short baselines (Schüler, 2005; Dong et al, 2016). For (2), apart from the problem of time delay in producing precise products (e.g., Kouba, 2015), most of the systematic errors cannot be modeled accurately (see also Sect. 2). In (3), parameterization is not always effective in estimating and mitigating the systematic errors due to problems of estimability and mismodeling. For (4), knowledge about the remaining systematic errors is usually insufficient to stochastically model them well.

We propose in this contribution a semiparametric estimation (SPE) approach to mitigate systematic errors in multiple GNSS positioning. Both simulated and real multiple GNSS datasets are used to validate the approach. The results show that the approach is effective, especially when applied before carrying out variance component estimation.

2 Impacts of systematic errors on multi-GNSS positioning

The linearized observation equation with systematic errors in the observations can be written as

$$\mathbf{L} = \mathbf{A}\mathbf{X} + \mathbf{S} + \boldsymbol{\varepsilon}, \quad E(\boldsymbol{\varepsilon}) = \mathbf{0}, \quad D(\boldsymbol{\varepsilon}) = \sigma^2 \mathbf{P}^{-1} \tag{1}$$

where $\mathbf{L} \in \mathbb{R}^m$, $\mathbf{A} \in \mathbb{R}^{m\times t}$, $\mathbf{X} \in \mathbb{R}^t$, $\mathbf{S} \in \mathbb{R}^m$, $\boldsymbol{\varepsilon} \in \mathbb{R}^m$, σ^2, and $\mathbf{P} \in \mathbb{R}^{m\times m}$ are the observations, design matrix, unknown parameters, systematic errors, observation errors, variance factor and weight matrix respectively; m and t are the number of observations and the number of unknown parameters respectively, with $m > t$; $E(\cdot)$ and $D(\cdot)$ denote the expectation and dispersion operators respectively. When $\mathbf{S} = \mathbf{0}$, Eq. (1) becomes the conventional parametric estimation model and can be resolved based on LS principle

$$\hat{\boldsymbol{\varepsilon}}^{\mathrm{T}} \mathbf{P} \hat{\boldsymbol{\varepsilon}} = \min \tag{2}$$

where $\hat{\boldsymbol{\varepsilon}}$ is the estimate of $\boldsymbol{\varepsilon}$, i.e., the vector of residuals. The LS solution can be expressed as

$$\hat{\mathbf{X}}_{\mathrm{LS}} = \mathbf{Q}_{\hat{\mathbf{X}}_{\mathrm{LS}}} \mathbf{A}^{\mathrm{T}} \mathbf{P} \mathbf{L}, \quad \mathbf{Q}^{-1}_{\hat{\mathbf{X}}_{\mathrm{LS}}} = \mathbf{N} = \mathbf{A}^{\mathrm{T}} \mathbf{P} \mathbf{A} \tag{3a}$$

$$\hat{\boldsymbol{\varepsilon}}_{\mathrm{LS}} = \mathbf{G}\mathbf{L}, \quad \mathbf{G} = \mathbf{I} - \mathbf{A}\mathbf{N}^{-1}\mathbf{A}^{\mathrm{T}}\mathbf{P} \tag{3b}$$

where $\hat{\mathbf{X}}_{\mathrm{LS}}$ is the estimated parameters with cofactor matrix $\mathbf{Q}_{\hat{\mathbf{X}}_{\mathrm{LS}}}$; $\hat{\boldsymbol{\varepsilon}}_{\mathrm{LS}}$ is the LS residuals; and $\mathbf{I}$ is an identity matrix. If $\mathbf{S} \neq \mathbf{0}$, the LS solution has the following biases

$$\mathbf{b}_{\hat{\mathbf{X}}_{\mathrm{LS}}} = \mathbf{N}^{-1}\mathbf{A}^{\mathrm{T}}\mathbf{P}\mathbf{S} \tag{4a}$$

$$\mathbf{b}_{\hat{\boldsymbol{\varepsilon}}_{\mathrm{LS}}} = \mathbf{G}\mathbf{S} \tag{4b}$$

where $\mathbf{b}_{\{.\}}$ represents the biases. Thus when systematic errors exist, the LS is biased and the estimated residuals are not random with zero mean.

Systematic errors can also impact on variance component estimation (VCE) that is based on the residuals (e.g., Xu et al, 2006). Considering that there are h types of observations in (1), i.e.,

$$\underset{m\times 1}{\mathbf{L}} = \{\underset{m_i\times 1}{\mathbf{L}_i}\}, \quad i \in \{1,2,\ldots,h\} \tag{5a}$$

$$D(\boldsymbol{\varepsilon}_i) = \sigma_i^2 \mathbf{P}_i^{-1}, \quad Cov(\boldsymbol{\varepsilon}_i, \boldsymbol{\varepsilon}_j) = \mathbf{0}, \quad (i \neq j) \tag{5b}$$

where $\mathbf{L}_i$ is the i-th subset with m_i observations in it; $\mathbf{P}_i$ is the weight matrix of $\mathbf{L}_i$; σ_i^2 is the variance component corresponding to $\mathbf{L}_i$; $Cov(\cdot)$ stands for the covariance operator. Here the observations from different subsets are assumed to be uncorrelated, leading to a block-diagonal weight matrix $\mathbf{P}$. The following Helmert VCE has been commonly used for weight determination in such cases (e.g., Koch and Kusche, 2002; Xu et al, 2006; Cai et al, 2014),

$$\hat{\boldsymbol{\theta}} = \boldsymbol{\Phi}^{-1}\boldsymbol{\Omega}, \quad \boldsymbol{\theta} = \{\sigma_i^2\}, \quad i \in \{1,2,\ldots,h\} \tag{6a}$$

$$\boldsymbol{\Phi}(i,i) = m_i - 2tr(\mathbf{N}^{-1}\mathbf{N}_i) + tr(\mathbf{N}^{-1}\mathbf{N}_i\mathbf{N}^{-1}\mathbf{N}_i) \tag{6b}$$

$$\boldsymbol{\Phi}(i,j) = tr(\mathbf{N}^{-1}\mathbf{N}_i\mathbf{N}^{-1}\mathbf{N}_j), \quad (i \neq j) \tag{6c}$$

$$\mathbf{N} = \sum_{i=1}^{h} \mathbf{N}_i, \quad \mathbf{N}_i = \mathbf{A}_i^{\mathrm{T}}\mathbf{P}_i\mathbf{A}_i \tag{6d}$$

$$\boldsymbol{\Omega}(i) = \hat{\boldsymbol{\varepsilon}}_i^{\mathrm{T}}\mathbf{P}_i\hat{\boldsymbol{\varepsilon}}_i \tag{6e}$$

where $\boldsymbol{\theta}$ denotes the vector of variance components to be estimated; and $tr(\cdot)$ is the matrix trace operator. VCE is carried out iteratively until the estimated variance factors converge.

When systematic errors are present in the observations, inserting (4b) into (6e) and (6a), one gets

$$\mathbf{b}_{\Omega}(i) = \mathbf{S}^{\mathrm{T}}\mathbf{G}_i^{\mathrm{T}}\mathbf{P}_i\mathbf{G}_i\mathbf{S} \tag{7a}$$

$$\mathbf{b}_{\hat{\theta}} = \boldsymbol{\Phi}^{-1}\mathbf{b}_{\Omega} \tag{7b}$$

where $\mathbf{b}_{\Omega}$ and $\mathbf{b}_{\hat{\theta}}$ represent the biases in the estimated $\boldsymbol{\Omega}$ and $\hat{\boldsymbol{\theta}}$, respectively; and $\mathbf{G}_i$ denotes the rows in $\mathbf{G}$ (see 3b) corresponding to the i-th subset of the observations. It is clear from the results that when systematic errors exist in the observations, $\boldsymbol{\Omega}$ is biased, resulting in biased variance components.

3 Semiparametric estimation (SPE)

3.1 SPE model

Eq. (1) has been commonly used as the functional model in SPE (see e.g., Fischer and Hegland, 1999; Jia, 2000; Ding et al, 2016). The model cannot be resolved by using the conventional LS approach due to the inclusion of unknowns $\mathbf{S}$. Instead, it can either be regularized to obtain a sub-optimal solution (see e.g., Green and Silverman, 1994), or add realistic prior information from a Bayesian viewpoint to generate an optimal solution (e.g., Fischer and Hegland, 1999; Koch and Kusche, 2002). The latter approach is not preferred when the true values of $\mathbf{S}$ are significantly different from zero (Xu and Rummel, 1994; Xu et al, 2006; Xu, 2009), although this is not considered a significant issue in GNSS relative positioning as the remaining systematic errors are in general close to zero after data pre-processing (e.g., differencing and applying corrections). For simplicity, we reduce the estimation to a generalized LS (GLS) problem (Menke, 2015), by using the prior information as pseudo observations ($\mathbf{S}$ is considered deterministic)

$$\mathbf{CS} + \boldsymbol{\varepsilon}_{\mathrm{c}} = \mathbf{0},\ E(\boldsymbol{\varepsilon}_{\mathrm{c}}) = \mathbf{0},\ D(\boldsymbol{\varepsilon}_{\mathrm{c}}) = \sigma^2\mathbf{P}_{\mathrm{c}}^{-1},\ Cov(\boldsymbol{\varepsilon}, \boldsymbol{\varepsilon}_{\mathrm{c}}) = \mathbf{0} \tag{8}$$

where $\mathbf{C} \in \mathbb{R}^{u\times m}$, $\boldsymbol{\varepsilon}_{\mathrm{c}} \in \mathbb{R}^{u}$ and $\mathbf{P}_{\mathrm{c}} \in \mathbb{R}^{u\times u}$ are respectively the design matrix, observation errors and weight matrix of the pseudo observations, with $u > t$. The systematic errors are also usually assumed to be smooth. The smoothness can be controlled by applying a discrete differentiation technique, e.g., making the second differences of $\mathbf{S}$ small (Green and Silverman, 1994, p. 76). Combining the prior information of both smoothness and magnitude of $\mathbf{S}$ gives

$$\mathbf{C} = \begin{bmatrix} \mathbf{F}_{\mathrm{d}} \\ \mathbf{I} \end{bmatrix},\ \text{where} \underset{(m-2)\times m}{\mathbf{F}_{\mathrm{d}}} = \mathrm{tridiag}(-0.5, 1, -0.5) \tag{9a}$$

$$\mathbf{P}_{\mathrm{c}} = \begin{bmatrix} \alpha\mathbf{P}_{\mathrm{d}} & \mathbf{0} \\ \mathbf{0} & \frac{\sigma^2}{\sigma_{\mathrm{s}}^2}\mathbf{I} \end{bmatrix} \tag{9b}$$

where $\mathbf{F}_{\mathrm{d}}$ is a second difference operator; α is a positive scalar called *smoothing parameter*; $\mathbf{P}_{\mathrm{d}}$ is a pre-given symmetric positive definite matrix, we empirically design it as $\mathbf{P}_{\mathrm{d}}(i,i) = \mathbf{P}(i+1, i+1), i \in \{1, 2, \ldots, m-2\}$; and σ_{s} represents the magnitude values of $\mathbf{S}$. Systematic errors of satellites with high elevations may be negligibly small and the corresponding parameters can be removed from the model by adjusting their σ_{s} to very small values. The magnitude prior information of $\mathbf{S}$ in (9) is sometimes necessary since uniquely solving (1) requires (Fischer and Hegland, 1999)

$$\mathrm{rank}(\mathbf{C}^{\mathrm{T}}\mathbf{P}_{\mathrm{c}}\mathbf{CA}) = t \tag{10}$$

In addition, the SPE model can become ill-posed due to over-parameterization and highly-correlated parameters. Using the magnitude pseudo observations is also more straightforward in preventing the ill-posedness compared with techniques such as truncated singular value decomposition and ridge regression (e.g., Xu, 1992, 1998; Hu, 2005). According to the GLS principle (Menke, 2015)

$$\hat{\boldsymbol{\varepsilon}}^{\mathrm{T}}\mathbf{P}\hat{\boldsymbol{\varepsilon}} + \hat{\boldsymbol{\varepsilon}}_{\mathrm{c}}^{\mathrm{T}}\mathbf{P}_{\mathrm{c}}\hat{\boldsymbol{\varepsilon}}_{\mathrm{c}} = \min \tag{11}$$

the GLS solution can be expressed as (Fischer and Hegland, 1999)

$$\hat{\mathbf{X}} = (\mathbf{A}^{\mathrm{T}}\mathbf{P}(\mathbf{I} - \mathbf{N}_{\mathrm{s}}^{-1}\mathbf{P})\mathbf{A})^{-1}\mathbf{A}^{\mathrm{T}}\mathbf{P}(\mathbf{I} - \mathbf{N}_{\mathrm{s}}^{-1}\mathbf{P})\mathbf{L} \tag{12a}$$

$$\hat{\mathbf{S}} = \mathbf{N}_{\mathrm{s}}^{-1}\mathbf{P}(\mathbf{L} - \mathbf{A}\hat{\mathbf{X}}), \quad \mathbf{N}_{\mathrm{s}} = \mathbf{P} + \mathbf{C}^{\mathrm{T}}\mathbf{P}_{\mathrm{c}}\mathbf{C} \tag{12b}$$

$$\mathbf{Q}_{\hat{\mathbf{X}}\hat{\mathbf{X}}} = \mathbf{N}^{-1} + \mathbf{N}^{-1}\mathbf{A}^{\mathrm{T}}\mathbf{P}\mathbf{Q}_{\hat{\mathbf{S}}\hat{\mathbf{S}}}\mathbf{PAN}^{-1} \tag{12c}$$

$$\mathbf{Q}_{\hat{\mathbf{S}}\hat{\mathbf{S}}} = (\mathbf{N}_{\mathrm{s}} - \mathbf{PAN}^{-1}\mathbf{A}^{\mathrm{T}}\mathbf{P})^{-1} \tag{12d}$$

In order to know the condition when SPE can improve the estimation accuracy, we compare mean square error (MSE) performances of the LS and GLS as follows, considering (3), (4) and (12c),

$$MSE(\hat{\mathbf{X}}_{\mathrm{LS}}) = \sigma^2 tr(\mathbf{Q}_{\hat{\mathbf{X}}_{\mathrm{LS}}}) + \mathbf{b}_{\hat{\mathbf{X}}_{\mathrm{LS}}}^{\mathrm{T}}\mathbf{b}_{\hat{\mathbf{X}}_{\mathrm{LS}}}$$
$$= \sigma^2 tr(\mathbf{N}^{-1}) + tr(\mathbf{N}^{-1}\mathbf{A}^{\mathrm{T}}\mathbf{PSS}^{\mathrm{T}}\mathbf{PAN}^{-1}) \tag{13a}$$

$$MSE(\hat{\mathbf{X}}) = \sigma^2 tr(\mathbf{Q}_{\hat{\mathbf{X}}\hat{\mathbf{X}}})$$
$$= \sigma^2 tr(\mathbf{N}^{-1} + \mathbf{N}^{-1}\mathbf{A}^{\mathrm{T}}\mathbf{P}\mathbf{Q}_{\hat{\mathbf{S}}\hat{\mathbf{S}}}\mathbf{PAN}^{-1}) \tag{13b}$$

if $\quad MSE(\hat{\mathbf{X}}_{\mathrm{LS}}) - MSE(\hat{\mathbf{X}}) > 0, \quad$ i.e.,

$$tr(\mathbf{N}^{-1}\mathbf{A}^{\mathrm{T}}\mathbf{P}(\mathbf{SS}^{\mathrm{T}} - \sigma^2\mathbf{Q}_{\hat{\mathbf{S}}\hat{\mathbf{S}}})\mathbf{PAN}^{-1}) > 0 \tag{13c}$$

we obtain

$$\mathbf{S}^{\mathrm{T}}\mathbf{S} > \sigma^2 tr(\mathbf{Q}_{\hat{\mathbf{S}}\hat{\mathbf{S}}}) \tag{13d}$$

It reveals that, the rationale behind the linear model expansion exists when significant systematic errors present in the data.

3.2 Determination of smoothing parameters

For the purpose of choosing the smoothing parameter α, numerical methods such as L-curve (Hansen, 1992) and generalized cross-validation (GCV) (Golub et al, 1979; Xu, 2009) are widely used. The L-curve method chooses the corner of an L-shaped curve consisting of norms of residuals and signals. It has been reported that the method produced an over-smoothed solution (Xu, 1998; Kusche and Klees, 2002). The GCV method uses a criterion that minimizes the norm of residuals of uncorrelated data (Green and Silverman, 1994, p. 71),

$$\mathrm{GCV}(\alpha) = \frac{\hat{\boldsymbol{\varepsilon}}^{\mathrm{T}}\mathbf{P}\hat{\boldsymbol{\varepsilon}}}{[tr(\mathbf{G}_{\mathrm{s}})/m]^2} = \frac{\mathbf{L}^{\mathrm{T}}\mathbf{G}_{\mathrm{s}}^{\mathrm{T}}\mathbf{P}\mathbf{G}_{\mathrm{s}}\mathbf{L}}{[tr(\mathbf{G}_{\mathrm{s}})/m]^2} \tag{14a}$$

where

$$\mathbf{G}_{\mathrm{s}} = \mathbf{I} - (\mathbf{I} - \mathbf{N}_{\mathrm{s}}^{-1}\mathbf{P})\mathbf{A}(\mathbf{A}^{\mathrm{T}}\mathbf{P}_{\mathrm{r}}\mathbf{A})^{-1}\mathbf{A}^{\mathrm{T}}\mathbf{P}_{\mathrm{r}} - \mathbf{N}_{\mathrm{s}}^{-1}\mathbf{P} \tag{14b}$$

$$\mathbf{P}_{\mathrm{r}} = \mathbf{P}(\mathbf{I} - \mathbf{N}_{\mathrm{s}}^{-1}\mathbf{P}) \tag{14c}$$

However, the determination of the smoothing parameter using the GCV or L-curve method, is time-consuming (Satirapod et al, 2003; Kusche and Klees, 2002).

The smoothing parameter α can also be interpreted as a weight-ratio (Kusche and Klees, 2002) and estimated through the VCE. We propose the following simplified procedure for enhancing the computation efficiency in determining the smoothing parameter based on the LS residuals (the conventional LS solution is derived beforehand):

(a) Estimate the approximate variances based on the LS residuals (see Appendix A for details, and we empirically configure $\mathbf{P}_{\mathrm{d}}$ as $\mathbf{P}_{\mathrm{d}}(i,i) = \mathbf{P}(i+1,i+1), i \in \{1,2,\ldots,m-2\}$),

$$\hat{\boldsymbol{\varepsilon}}_{\mathrm{d}} = \mathbf{F}_{\mathrm{d}}\hat{\mathbf{S}} \approx \mathbf{F}_{\mathrm{d}}\mathbf{F}_{\mathrm{L}}\hat{\boldsymbol{\varepsilon}}_{\mathrm{LS}}, \quad \hat{\boldsymbol{\varepsilon}} \approx \mathbf{F}_{\mathrm{H}}\hat{\boldsymbol{\varepsilon}}_{\mathrm{LS}} \tag{15a}$$

$$\hat{\sigma}_{\mathrm{d}}^2 = \gamma_{\mathrm{d}}\frac{\hat{\boldsymbol{\varepsilon}}_{\mathrm{d}}^{\mathrm{T}}\hat{\boldsymbol{\varepsilon}}_{\mathrm{d}}}{m-2} \approx \gamma_{\mathrm{d}}\frac{\hat{\boldsymbol{\varepsilon}}_{\mathrm{LS}}^{\mathrm{T}}\mathbf{F}_{\mathrm{L}}^{\mathrm{T}}\mathbf{F}_{\mathrm{d}}^{\mathrm{T}}\mathbf{F}_{\mathrm{d}}\mathbf{F}_{\mathrm{L}}\hat{\boldsymbol{\varepsilon}}_{\mathrm{LS}}}{m-2} \tag{15b}$$

$$\hat{\sigma}^2 = \gamma\frac{\hat{\boldsymbol{\varepsilon}}^{\mathrm{T}}\hat{\boldsymbol{\varepsilon}}}{m-1} \approx \gamma\frac{\hat{\boldsymbol{\varepsilon}}_{\mathrm{LS}}^{\mathrm{T}}\mathbf{F}_{\mathrm{H}}^{\mathrm{T}}\mathbf{F}_{\mathrm{H}}\hat{\boldsymbol{\varepsilon}}_{\mathrm{LS}}}{m-1} \tag{15c}$$

where $\mathbf{F}_{\mathrm{L}} \in \mathbb{R}^{m\times m}$ and $\mathbf{F}_{\mathrm{H}} \in \mathbb{R}^{(m-1)\times m}$ are the low-pass and high-pass filter operation matrices given in (A.3) and (A.6), respectively; γ and γ_{d} are positive scalars that represent the errors in $\hat{\sigma}_{\mathrm{d}}$ and $\hat{\sigma}$ caused by the simplification, respectively.

(b) Finally, assuming $\gamma \approx \gamma_{\mathrm{d}}$, the approximate smoothing parameter can be calculated,

$$\hat{\alpha} = \frac{\hat{\sigma}^2}{\hat{\sigma}_{\mathrm{d}}^2} \approx \frac{m-2}{m-1}\frac{\hat{\boldsymbol{\varepsilon}}_{\mathrm{LS}}^{\mathrm{T}}\mathbf{F}_{\mathrm{H}}^{\mathrm{T}}\mathbf{F}_{\mathrm{H}}\hat{\boldsymbol{\varepsilon}}_{\mathrm{LS}}}{\hat{\boldsymbol{\varepsilon}}_{\mathrm{LS}}^{\mathrm{T}}\mathbf{F}_{\mathrm{L}}^{\mathrm{T}}\mathbf{F}_{\mathrm{d}}^{\mathrm{T}}\mathbf{F}_{\mathrm{d}}\mathbf{F}_{\mathrm{L}}\hat{\boldsymbol{\varepsilon}}_{\mathrm{LS}}} \tag{16}$$

3.3 Hypothesis test for systematic errors

Hypothesis test can be carried out to examine the significance of the systematic errors, using techniques such as model validations (Teunissen, 1998; Leick et al, 2015) and Durbin-Watson method (Jia et al, 2002). If no significant systematic error is detected, the corresponding nonparametric term s can be eliminated, or equivalently, fix s to zero. To simplify the computation, the following procedure is adopted to detect systematic errors in the observations from individual satellites based on the LS residuals (outliers have been screened). The null and alternative hypotheses are,

$$\mathbf{H}_0 : E(\hat{\sigma}_{\mathrm{a}}^2) = E(\hat{\sigma}_{\mathrm{r}}^2) \quad \text{against} \quad \mathbf{H}_1 : E(\hat{\sigma}_{\mathrm{a}}^2) < E(\hat{\sigma}_{\mathrm{r}}^2) \tag{17}$$

where $\hat{\sigma}_{\mathrm{a}}^2 = \frac{1}{2(m-1)}\sum_{i=1}^{m-1}(v_{i+1}-v_i)^2$, and $\hat{\sigma}_{\mathrm{r}}^2 = \frac{1}{m}\sum_{i=1}^{m} v_i^2$. The ratio between them satisfies the following distribution when there are enough samples (e.g., $m > 20$) (Zar, 2009),

$$\frac{\hat{\sigma}_{\mathrm{a}}^2}{\hat{\sigma}_{\mathrm{r}}^2} \sim \mathrm{N}(1, \frac{1}{m+1}) \tag{18}$$

A Z-test statistic can thus be calculated,

$$z = \sqrt{m+1}(1 - \frac{\hat{\sigma}_{\mathrm{a}}^2}{\hat{\sigma}_{\mathrm{r}}^2}) \sim \mathrm{N}(0,1) \tag{19}$$

We choose to use a rejection region $z > z_{0.99}$ (a critical value of standard normal distribution with significance level 0.01). This relatively high significance level is chosen as it helps to reduce the risk of introducing too many unknown parameters when modeling the systematic errors.

4 Processing multiple GNSS data with SPE

A multiple GNSS double-difference (DD) carrier phase observation can be expressed as (e.g., Wang et al, 2001)

$$L^{ij}(k) = \rho^{ij}(k) + \lambda^i N^{ij} + (\lambda^i - \lambda^j)N^j + \varepsilon^{ij}(k) \tag{20}$$

where $L^{ij}(k)$ is the DD carrier phase (scaled to meters) of satellite pair i-j at epoch k; j indicates the reference satellite; ρ is the geometric distance; λ is the wavelength; N is the phase ambiguity, including DD ambiguity N^{ij}, and single-difference (SD) ambiguity N^j that cannot be canceled out in multi-frequency case. Approximate SD ambiguities are usually calculated from pseudoranges and more accurate SD are estimated when fixing the DD ambiguities; and ε is the observation error.

A term representing possible systematic errors can be added to the DD observation equation in (20). Since the systematic errors may be absorbed partially by the float ambiguities (Wang et al, 2001; Xu, 2006), it is necessary to remove the systematic errors before fixing the ambiguities. The DD observation equation becomes

$$L^{ij}(k) = \rho^{ij}(k) + \lambda^i N^{ij} + (\lambda^i - \lambda^j)N^j + s^{ij}(k) + \varepsilon^{ij}(k) \tag{21}$$

where s is the parameter representing the systematic errors that may depend on the satellites, site and time.

GNSS data processing requires vector semiparametric models (Fessler, 1991; Jia, 2000) sine the observations contain a set of satellites. Assuming that n_{sat} satellites are tracked simultaneously for m epochs, and denoting n_{ref} as the number of reference satellites (a reference satellite is selected for each satellite system involved) and n as the number of smoothing parameters ($n = n_{sat} - n_{ref}$), $m \times n$ additional parameters need to be estimated. Criterion in (11) can be extended into

$$\begin{cases} \sum_{k=1}^{m} \underset{1\times n}{\hat{\boldsymbol{\varepsilon}}_k^{\mathrm{T}}} \mathbf{P}_k \hat{\boldsymbol{\varepsilon}}_k + \underset{1\times mn}{\hat{\bar{\mathbf{S}}}^{\mathrm{T}}} \bar{\mathbf{C}}^{\mathrm{T}} \bar{\mathbf{P}}_{\mathrm{c}} \bar{\mathbf{C}} \hat{\bar{\mathbf{S}}} = \min \\ \underset{mn\times 1}{\bar{\mathbf{S}}} = \{ \underset{n\times 1}{\mathbf{S}_k} \}, \quad k \in \{1, 2, \ldots, m\} \\ \bar{\mathbf{C}} = \underset{u\times m}{\mathbf{C}} \otimes \underset{n\times n}{\bar{\alpha}^{\frac{1}{2}}} \\ \bar{\mathbf{P}}_{\mathrm{c}} = \text{block-diag}(\mathbf{P}_{\mathrm{c},1}, \mathbf{P}_{\mathrm{c},2}, \cdots, \mathbf{P}_{\mathrm{c},m}) \\ \bar{\alpha} = \mathrm{diag}(\alpha_1, \alpha_2, \cdots, \alpha_n) \end{cases} \tag{22}$$

where m and n are respectively the number of observation epochs and the number of smoothing parameters as mentioned above; u, $\mathbf{C}$ and $\mathbf{P}_{\mathrm{c},k}$ are respectively the number, design matrix and weight matrix of the pseudo observations defined in (8); k is the epoch index; and $\otimes$ is the Kronecker operator.

5 Experimental results

Two experiments (one with simulated and one with real multiple GNSS data) are carried out to investigate the performance of the proposed SPE approach when combined with VCE in processing the GNSS data. For simplicity, the combined use of SPE and VCE will be referred to hereafter as SVE (Semiparameter and Variance Estimation). For comparison, conventional LS estimation and VCE based on results from the conventional LS are also carried out. In the conventional LS estimation, the inter-system weight-ratios are set equal to 1. The SPE is carried out before the VCE. A smoothing parameter is added for each satellite pair and adjusted individually based on Eq. (16). SVE is applied in both float and ambiguity fixed solutions.

The results are evaluated with the aforementioned Z-test and the following baseline quality indicators (Blewitt, 1989),

$$\text{Length error} = \left(\delta_N^2 + \delta_E^2 + \delta_U^2\right)^{\frac{1}{2}} \tag{23a}$$

$$\text{Repeatability}(\delta) = \left(\frac{\sum_{i=1}^{n_s} \delta_i^2 / \sigma_{\delta_i}^2}{\sum_{i=1}^{n_s} 1/\sigma_{\delta_i}^2} \right)^{\frac{1}{2}} \tag{23b}$$

where δ stands for baseline errors with respect to the truths, with subscripts N, E and U denoting the corresponding north, east and up coordinate components; i indicates the session number (n_s in total); and σ_δ is the standard deviation (STD) of δ.

LAMBDA method (Teunissen, 1995) is used in all the above three methods for ambiguity resolution with R-ratio as the validation indicator (Euler and Schaffrin, 1991). More recent progress in the ambiguity resolution can be found in (e.g., Chang et al, 2005; Xu et al, 2012). The computer time is recorded to assess the computation efficiency and to show the advantages of the proposed simplified SPE approach. Different SVEs are carried out, including those based on the traditional iterative and search methods discussed above, i.e., the VCE and GCV (with and without magnitude prior information where the latter is referred to as *GCV-free*). The Golden Section technique (Press et al, 2007) is applied in the search process of the GCV (in the range from 10^{-15} to 10^{15}). Note that the GCV-free SVE is used only in the fixed-ambiguity solution as (10) is violated when the design matrix $\mathbf{A}$ is based on (21), and Eq. (9) only contains the smoothness of $\mathbf{S}$ (i.e., $\mathbf{C} = \mathbf{F}_{\mathrm{d}}$ and $\mathbf{P}_{\mathrm{c}} = \alpha \mathbf{P}_{\mathrm{d}}$). Initial values of the smoothing parameters in the SVE are computed by the approximate formula (16) to accelerate the convergence.

5.1 Experiment with simulated data

Sinusoidal systematic errors (in cycles) are simulated using Eq. (24) and added to the raw GNSS observations over a zero-baseline. The session length is three hours with a data sampling interval of 90 s (a relatively large interval being used to reduce the computation load). The dataset contains L1/B1/G1 observations from 9/9/7 satellites of G/C/R (hereafter G, C and R stand for GPS, Beidou and GLONASS respectively). The systematic errors simulated have different periods (1.5 h for G12, 2.5 h for both G22 and C02) but the same amplitudes (0.05 cycles),

$$\begin{cases} \text{G12} : 0.05 \sin\left(\dfrac{tow}{1.5 \times 3600} 2\pi\right) \\ \text{G22} : 0.05 \sin\left(\dfrac{tow}{2.5 \times 3600} 2\pi\right) \\ \text{C02} : 0.05 \sin\left(\dfrac{tow}{2.5 \times 3600} 2\pi\right) + 0.1 \end{cases} \tag{24}$$

where tow is time of week in seconds. A constant offset of 0.1 cycles is also added to C02. When applying the SPE, we set the standard deviations of the standard deviations of the pseudo observations to 0.2 cycles (a relatively loose constraint to avoid possible distortion of the results), i.e., $\sigma_s = 0.2 \times \text{wavelength}$ in (9).

Fig. 1 shows the length errors of the baseline from the different estimators. It can be seen that the simulated systematic errors have introduced nearly up to 7 mm length error to the zero-baseline. The VCE method then reduces this discrepancy to 3 mm through raising GLONASS's weight from 1.0 to 2.9 (see Table 1), while this improvement is achieved at the cost of roughly down-weighting the observations from all the other satellites, both GPS and Beidou, including those without systematic errors. Compared with the results of VCE that based on raw data (see Table 1), apparently the weight ratios are seriously falsified as the Z-test statistics are all increased. The SVE approach has significantly reduced the length error to about 0.5 mm (over 90% improvement compared with LS, and over 80% compared with VCE), and improved the R-ratio from 16.4 to 58.5, indicating a much more reliable solution. The weight ratios obtained by SVE are closer to those obtained based on the raw data without systematic errors. Fig. 2 shows the residuals from the different solutions. It is clear that LS and VCE do not cope with the systematic errors well. The SVE models much better the systematic errors and the residuals become more random, all the residuals have finally passed the Z-test (see Table 1). According to the Z-test results, SVE works better with low-frequency systematic errors than high-frequency errors. The LS residuals may appear very inconsistent at times, particularly in Fig. 2c where an offset clearly exists between them.

In order to understand the performances when using different SVEs, we compare the results of different session lengths (from 0.5 h to 3.0 h, increasing 0.5 h gradually). As shown in Fig. 3, the baseline accuracy obtained by the simplified approach are similar to those obtained based on VCE and GCV, and they are superior to those using the GCV-free method. The advantage of adding prior information on the magnitude of the systematic errors is more evident in sessions of shorter lengths (with weaker model strength), where the results based on GCV-free approach are dramatically deteriorated. The computation efficiency of the simplified procedure is also proved to be advantageous. The time consumption of the GCV-based SVEs raises exponentially as the session length increases. The VCE-based SVE reduces the mean calculation time from about 9 h to less than 3 h (see Table 2) while the simplified approach further shortens it by almost 30 times to about 0.1 h (i.e., almost 100 times faster than the GCV-based procedures).

These results indicate that, compared with conventional search and iterative algorithms, the simplified approach can achieve comparable baseline solutions with a considerably higher efficiency.

5.2 Experiments with real datasets

The multi-GNSS dataset consists of GPS/Beidou single frequency (L1/B1) observations covering three consecutive days (day 320 to 322 in year 2014). It is from a baseline of about 10 m on the roof of Wenfa Building at The Central South University, China. The points are referred to as CSUA and CSUB respectively. A reflective environment was created by placing tinfoil paper on the north wall near site CSUA and therefore the multipath signals are considered strong (Fig. 4). The observations were divided equally into 24 sessions, and each session was sampled at 90 s to reduce the computation load. Observations below elevation angle of 10° were not used. The baseline components are estimated based on all the GPS data and used as the truths in evaluating the performances of the methods. In SPE, the systematic errors are empirically constrained to be within 0.15 cycles. (three times as large as the normal amplitude of DD phase residuals in short baselines, i.e. 0.05 cycles).

Fig. 5 shows the sky plots and signal strengths. It can be seen that the satellite signals (especially GPS) from the north direction were blocked significantly and have much lower signal strength. Beidou system contributes more to both the number of the satellites and the signal quality (Fig. 5b).

Fig. 6 illustrates the time series of L1/B1 C/A code multipath combination (e.g., Shi et al, 2013) from data of different types of satellites. As the multipath signals increase with descending elevations, the Median Earth Orbit (MEO) G31 (Fig. 6a) with a bell-shaped elevation pattern has larger multipath effect at the two ends. The effect becomes smaller at the two peak elevations of the camelback-shaped Inclined Geosynchronous Orbit (IGSO) C10 (Fig. 6b). The elevation of the Geosynchronous Orbit (GEO) C05 (Fig. 6c) varies slowly in a sinusoidal pattern and its multipath effects were more stable compared with those of the MEO and IGSO. Signals from GEO presented a higher continuity as it stayed on the southern sky, those from MEO and IGSO were partially shadowed by the northern wall (Fig. 4) when they traveled to the back side (during the hours of about 14–17 for G31, and about 15–19 for C10 respectively). More frequent and larger multipath errors can be seen near about 60° elevation when the satellites were nearly blocked.

Fig. 7 shows the length errors of the baseline from the different processing methods. It can be seen that compared with LS, the VCE approach has produced lower baseline errors in 14 out of 24 of the observation sessions. As shown in Table 3, the length repeatability is improved by 19.4% by the VCE approach as Beidou's mean weight is increased by 4.1 times. The SVE solution has further improved the length repeatability by 35.6% when adjusting Beidou's mean weight to 1.8. For both VCE and SVE, significant improvements can be seen in the north and vertical directions, while the repeatability of the east component is lowered slightly by the SVE approach. The R-ratios are improved by using the SVE approach in the ambiguity resolution.

The VCE-based SVE approach has produced similar baseline solutions as those of the simplified approach, with the differences between the baseline components being smaller than 0.1 mm. The results are superior than those produced by GCV-based SVE. Results from GCV-free SVE are not presented here due to its unsatisfactory performance (see Sect. 5.1). A great advantage of the proposed simplified approach is in its high computation efficiency. The average computation time (see Table 2 for the configuration of the PC used) used for a baseline solution (session length is 3 hours) is 0.1 h, over 20 times faster than the VCE-based SVE, and over 100 times faster than the GCV-based SVE.

We select the 5-th session to show some further details of the results. The number of satellites in view is relatively less in this session and there appear apparently some systematic errors in the GNSS observations. The DD residuals from the LS and the SVE solutions as well as the systematic errors estimated from the SVE solution are shown in Fig. 8, and some statistics of the residuals are given in Fig. 9. The residuals from standard LS and VCE approaches are not presented here as they cannot resist the systematic errors so that the results are not very satisfactory. From the residuals shown in Fig. 8a, it is apparent that there exist some significant systematic errors varying over time. For example, residuals from G31-G22 and C10-C03 satellite pairs fluctuated obviously over time, and those from C05-C03 are fairly constant. After the SVE approach is applied, systematic errors in the LS residuals have been accurately estimated (Fig. 8b) and removed. Therefore residuals from the SVE solution appear much more random (Fig. 8c) with both the biases and the STDs being significantly reduced (see Fig. 9). The results clearly indicate that the proposed SPE approach is effective in mitigating the systematic errors and that the application of the approach can significantly improve the results of VCE.

Three typical satellites of different orbits are selected to assess the performances of SVE and LS. The residuals from the experiments are given in Fig. 10, the corresponding Z-test statistics and the smoothing parameters (both from float and fixed ambiguity solutions) from the SVE are given in Table 4. It can be seen that by extracting the systematic errors, the mean of the residuals becomes much closer to zero and the histogram of the residuals is more concentrated around the center. Similar improvements can be seen in the results of the Z-test where the test statistics decrease significantly and the residuals of most of the satellite-pairs pass the test. In addition, systematic errors with larger magnitudes are generally penalized with smaller smoothing parameters (when use the z statistic as an indicator in the analysis, the numbers of the observations should be similar). The smoothing parameters of the float-ambiguity solution are similar to those from the fixed-ambiguity solution except those set to large values because their residuals from the float solution pass the Z-test. For some satellite pairs (e.g., G31-G22 in Fig. 10a), the high frequency systematic errors still remain although the magnitudes are small. There are apparent inconsistencies between the estimated systematic errors and the LS-derived residuals (e.g. C05-C03 in Fig. 10c). This indicates that (see also Fig. 2c), it is sometimes not appropriate to determine the systematic errors based on the residuals.

6 Discussions and Conclusions

A semiparametric estimation (SPE) based approach has been proposed for processing observations from multiple GNSS. Results from a zero-baseline (GPS/Beidou/GLONASS) experiment have shown that systematic errors can be accurately estimated based on the proposed approach. The approach when combined with VCE can significantly improve the accuracy of variance component estimation and the accuracy of the baseline (over 80% improvement compared to results of VCE and over 90% improvement over the results of LS). Experiments using a real dataset gathered from a GPS/Beidou baseline of about 10 m in a multipath dominant environment have shown a 35.6% improvement in accuracy when SPE was applied. The determination of the smoothing parameters used in the SPE based on search algorithms like generalized cross-validation (GCV) is computationally intensive. A method based on LS residuals has been proposed for this purpose and has been proved practical and effective.

There are issues about the proposed SPE approach that are worth of further study. For example, it will be interesting to apply the proposed SPE approach to dynamic applications where more challenging issues such as the changing observation environments may be encountered. Robust SPE may also be developed to cope with gross errors.

Acknowledgements The authors would like to thank the anonymous reviewers and the editors for their constructive comments. Mr. Xiao Gao helped with collecting the test dataset at campus of The Central South University. Discussions with Prof. Bofeng Li of Tongji University are very useful. The research was partly supported by the Research Grants Council of Hong Kong (Proj. No. E-PolyU501/16), National Natural Science Foundation of China (Proj. No. 41374013), and special fund for public projects of National Administration of Surveying, Mapping and Geoinformation of China (Proj. No. 201412016).

Appendix A : Estimation of the signal and variance

Considering the following data series,

$$y(i) + e(i) = s(i), \quad i \in \{1, 2, \ldots, m\} \tag{A.1}$$

where s is an m data-point signal that varies slowly in time; e is a white noise series with variance σ^2.

(1) Applying a low-pass filter operation, typically using the following slide window average technique, the signal can be extracted,

$$\hat{s}(i) = \frac{1}{2w+1} \sum_{j=i-w}^{i+w} y(j) \tag{A.2}$$

where w is the window size at the ith data point. Therefore an $(m \times m)$ low-pass filter operation matrix can be obtained as (w_0 is a given window size),

$$\mathbf{F}_{\mathrm{L}}(i,j) = (2w+1)^{-1}, \quad (i-w \leqslant j \leqslant i+w) \tag{A.3a}$$

$$w = \begin{cases} i-1, & (1 \le i \le w_0) \\ m-i, & (m-w_0+1 \le i \le m) \\ w_0, & \text{otherwise} \end{cases} \tag{A.3b}$$

(2) Using a high-pass filter operation to remove the signal, e.g., the first difference,

$$\hat{e}(i) = \frac{y(i+1)-y(i)}{\sqrt{2}}, \quad i \in \{1,2,\cdots,m-1\} \tag{A.4}$$

then the variance is estimated via the following mean square successive difference (Zar, 2009), which is insensitive to the signal,

$$\hat{\sigma}^2 = \frac{1}{(m-1)} \sum_{i=1}^{m-1} \hat{e}(i)^2 \tag{A.5}$$

The $(m-1)\times m$ corresponding difference operation matrix is

$$\mathbf{F}_{\mathrm{H}} = \mathrm{bidiag}(-\frac{1}{\sqrt{2}}, \frac{1}{\sqrt{2}}) \tag{A.6}$$

References

Blewitt G (1989) Carrier phase ambiguity resolution for the global positioning system applied to geodetic baselines up to 2000 km. J Geophys Res: Solid Earth 94(B8):10,187–10,203, DOI 10.1029/JB094iB08p10187

Cai C, Pan L, Gao Y (2014) A precise weighting approach with application to combined L1/B1 GPS/BeiDou positioning. J Navig 67:911–925, DOI 10.1017/S0373463314000320

Chang X, Yang X, Zhou T (2005) MLAMBDA: a modified LAMBDA method for integer least-squares estimation. J Geod 79(9):552–565, DOI 10.1007/s00190-005-0004-x

Ding S, Shi J, Jiang W (2016) Theory and method of hypothetical test for nonparameters in linear semiparametric model. Surv Rev 0(0):1–6, DOI 10.1179/1752270614Y.0000000147

Dong D, Wang M, Chen W, Zeng Z, Song L, Zhang Q, Cai M, Cheng Y, Lv J (2016) Mitigation of multipath effect in GNSS short baseline positioning by the multipath hemispherical map. J Geod 90(3):255–262, DOI 10.1007/s00190-015-0870-9

Euler HJ, Schaffrin B (1991) On a measure for the discernibility between different ambiguity solutions in the static-kinematic GPS-mode. In: Schwarz KP, Lachapelle G (eds) Kinematic Systems in Geodesy, Surveying, and Remote Sensing: Symposium No. 107 Banff, Alberta, Canada, September 10–13, 1990, Springer New York, pp 285–295, DOI 10.1007/978-1-4612-3102-8_26

Fessler JA (1991) Nonparametric fixed-interval smoothing with vector splines. IEEE Trans Signal Process 39(4):852–859, DOI 10.1109/78.80907

Fischer B, Hegland M (1999) Collocation, filtering and nonparametric regression, part i. ZFV 124(1):17–24

Golub GH, Heath M, Wahba G (1979) Generalized cross-validation as a method for choosing a good ridge parameter. Technometrics 21(2):215–223, DOI 10.1080/00401706.1979.10489751

Green PJ, Silverman BW (1994) Nonparametric regression and generalized linear models: a roughness penalty approach. CRC Press, London

Hansen PC (1992) Analysis of discrete ill-posed problems by means of the L-curve. SIAM Rev 34(4):561–580, DOI 10.1137/1034115

Hofmann-Wellenhof B, Lichtenegger H, Wasle E (2008) GNSS: Global Navigation Satellite Systems: GPS, GLONASS, Galileo, and More. Springer-Verlag Wien

Hoque MM, Jakowski N (2007) Higher order ionospheric effects in precise GNSS positioning. J Geod 81(4):259–268, DOI 10.1007/s00190-006-0106-0

Hu H (2005) Ridge estimation of a semiparametric regression model. J Comput Appl Math 176(1):215–222, DOI 10.1016/j.cam.2004.07.032

Jia M (2000) Mitigation of systematic errors of GPS positioning using vector semiparametric models. In: Proc. ION GPS, pp 1938–1947

Jia M, Stewart M, Tsakiri M (2002) A statistical test procedure for the detection and identification of GPS systematic errors. In: Ádám J, Schwarz KP (eds) Vistas for Geodesy in the New Millennium: IAG 2001 Scientific Assembly, Budapest, Hungary September 2–7, 2001, Springer Berlin Heidelberg, Berlin, Heidelberg, pp 404–409, DOI 10.1007/978-3-662-04709-5_67

Koch KR, Kusche J (2002) Regularization of geopotential determination from satellite data by variance components. J Geod 76(5):259–268, DOI 10.1007/s00190-002-0245-x

Kouba J (2015) A guide to using International GNSS Service (IGS) products. URL https://igscb.jpl.nasa.gov/igscb/resource/pubs/UsingIGSProductsVer21_cor.pdf, accessed: 2015-11-11

Kusche J, Klees R (2002) Regularization of gravity field estimation from satellite gravity gradients. J Geod 76(6):359–368, DOI 10.1007/s00190-002-0257-6

Leick A, Rapoport L, Tatarnikov D (2015) GPS Satellite Surveying, 4th edn. John Wiley and Sons, Inc, DOI 10.1002/9781119018612

Li X, Ge M, Dai X, Ren X, Fritsche M, Wickert J, Schuh H (2015) Accuracy and reliability of multi-GNSS real-time precise positioning: GPS, GLONASS, BeiDou, and Galileo. J Geod 89(6):607–635, DOI 10.1007/s00190-015-0802-8

Meng X, Roberts GW, Dodson AH, Cosser E, Barnes J, Rizos C (2004) Impact of GPS satellite and pseudolite geometry on structural deformation monitoring: analytical and empirical studies. J Geod 77(12):809–822, DOI 10.1007/s00190-003-0357-y

Menke W (2015) Review of the generalized least squares method. Surv Geophys 36(1):1–25, DOI 10.1007/s10712-014-9303-1

Paziewski J, Wielgosz P (2015) Accounting for Galileo-GPS intersystem biases in precise satellite positioning. J Geod 89(1):81–93, DOI 10.1007/s00190-014-0763-3

Press WH, Teukolsky SA, Vetterling WT, Flannery BP (2007) Numerical recipes: The art of scientific computing, 3rd edn. Cambridge university press

Satirapod C, Wang J, Rizos C (2003) Comparing different GPS data processing techniques for modelling residual systematic errors. J Surv Eng 129(4):129–135

Schüler T (2005) Impact of systematic errors on precise long baseline kinematic GPS positioning. GPS Solut 10(2):108–125, DOI 10.1007/s10291-005-0012-6

Shi C, Zhao Q, Hu Z, Liu J (2013) Precise relative positioning using real tracking data from Compass GEO and IGSO satellites. GPS Solut 17(1):103–119, DOI 10.1007/s10291-012-0264-x

Teunissen P (1995) The least-squares ambiguity decorrelation adjustment: a method for fast GPS integer ambiguity estimation. J Geod 70(1-2):65–82, DOI 10.1007/BF00863419

Teunissen P (1998) Quality control and GPS. In: Teunissen P, Kleusberg A (eds) GPS for Geodesy, Springer Berlin Heidelberg, pp 271–318, DOI 10.1007/978-3-642-72011-6_7

Teunissen P, Odolinski R, Odijk D (2014) Instantaneous BeiDou+GPS RTK positioning with high cut-off elevation angles. J Geod 88(4):335–350, DOI 10.1007/s00190-013-0686-4

Tian Y, Ge M, Neitzel F (2015) Particle filter-based estimation of inter-frequency phase bias for real-time GLONASS integer ambiguity resolution. J Geod pp 1–14, DOI 10.1007/s00190-015-0841-1

Wang J, Rizos C, Stewart MP, Leick A (2001) GPS and GLONASS integration: Modeling and ambiguity resolution issues. GPS Solut 5(1):55–64, DOI 10.1007/PL00012877

Wanninger L (2012) Carrier-phase inter-frequency biases of GLONASS receivers. J Geod 86(2):139–148, DOI 10.1007/s00190-011-0502-y

Xu P (1991) Least squares collocation with incorrect prior information. Zfv 116:266–273

Xu P (1992) Determination of surface gravity anomalies using gradiometric observables. Geophys J Int 110(2):321–332, DOI 10.1111/j.1365-246X.1992.tb00877.x

Xu P (1998) Truncated SVD methods for discrete linear ill-posed problems. Geophys J Int 135(2):505–514, DOI 10.1046/j.1365-246X.1998.00652.x

Xu P (2006) Voronoi cells, probabilistic bounds, and hypothesis testing in mixed integer linear models. IEEE Trans Inf Theory 52(7):3122–3138, DOI 10.1109/TIT.2006.876356

Xu P (2009) Iterative generalized cross-validation for fusing heteroscedastic data of inverse ill-posed problems. Geophys J Int 179(1):182–200, DOI 10.1111/j.1365-246X.2009.04280.x

Xu P, Rummel R (1994) Generalized ridge regression with applications in determination of potential fields. Manuscripta Geodaetica 20(1):8–20

Xu P, Shen Y, Fukuda Y, Liu Y (2006) Variance component estimation in linear inverse ill-posed models. J Geod 80(2):69–81, DOI 10.1007/s00190-006-0032-1

Xu P, Shi C, Liu J (2012) Integer estimation methods for GPS ambiguity resolution: an applications oriented review and improvement. Surv Rev 44(324):59–71, DOI 10.1179/1752270611Y.0000000004

Yang Y, Li J, Xu J, Tang J, Guo H, He H (2011) Contribution of the Compass satellite navigation system to global PNT users. Chin Sci Bull 56(26):2813–2819, DOI 10.1007/s11434-011-4627-4

Ye S, Chen D, Liu Y, Jiang P, Tang W, Xia P (2014) Carrier phase multipath mitigation for BeiDou navigation satellite system. GPS Solut 19(4):545–557, DOI 10.1007/s10291-014-0409-1

Zar JH (2009) Serial randomness of measurements: parametric testing. In: Biostatistical analysis, 5th edn, Pearson, pp 599–601

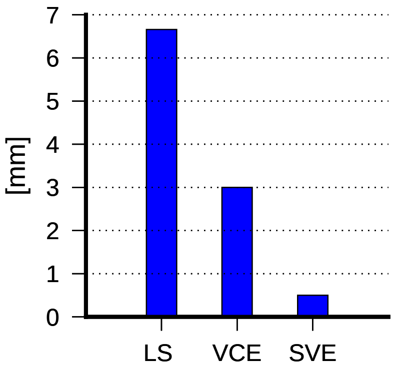

Fig. 1 Baseline length errors from different estimators (observation session length: 3 h)

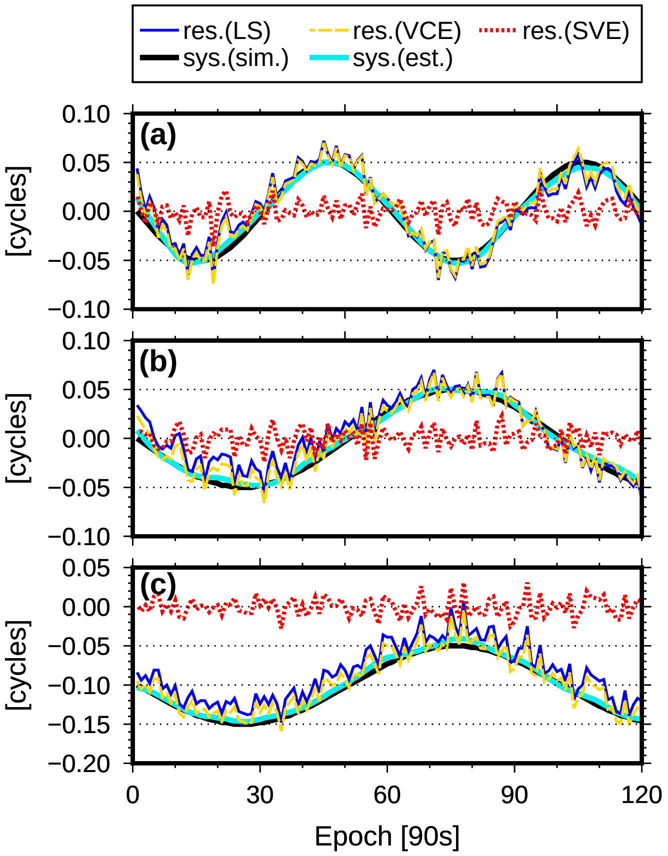

Fig. 2 Residuals of (a) G12-G18, (b) G22-G18 and (c) C02-C07 estimated by the different estimators, and systematic errors simulated and estimated by SVE (observation session length: 3 h); Here 'res.', 'sim.', 'sys.' and 'est.' represent 'residuals', 'simulated', 'systematic errors' and 'estimated', respectively

Table 1 Solutions of zero baseline with simulated systematic errors from different estimators (session length: 3 h)

	LS	VCE	VCE (raw data)	SVE
Baseline bias (X/Y/Z) [mm]	-4.6/3.2/3.6	-1.8/1.8/1.6	-0.1/0.4/-0.1	-0.4/0.0/0.3
Weight-ratio (G/C/R)	1.0/1.0/1.0	1.0/0.4/2.9	1.0/0.5/0.6	1.0/0.4/0.7
R-Ratio	16.4	16.4	>1000.0	58.5
Z-test (z): G12-G18	10.0	10.0	1.6*	-0.4*
Z-test (z): G22-G18	9.8	9.8	-0.3*	-2.2*
Z-test (z): C02-C07	10.8	10.8	-0.1*	-1.0*

* Residuals that passed the Z-test (significance level 0.01)

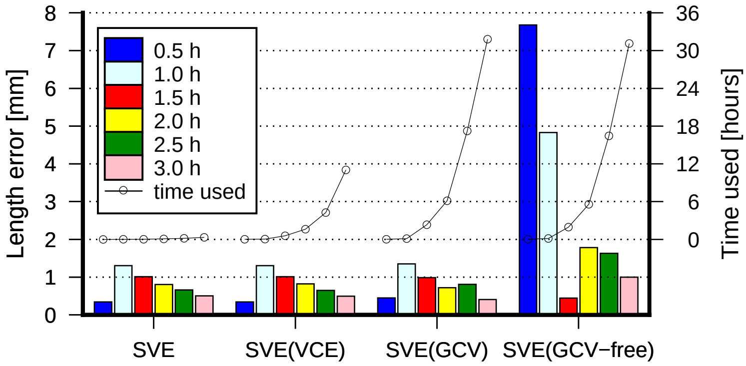

Fig. 3 Baseline length errors from different semiparametric estimators and different observation session lengths

Table 2 Solutions of the simulated zero-baseline and systematic errors from different semiparametric estimators (session lengths: 0.5,1.0,$\cdots$,3.0 h)

Mean value	SVE	SVE (VCE)	SVE (GCV)	SVE (GCV-free)
Length error [mm]	0.8	0.8	0.8	2.9
R-Ratio	36.3	36.2	23.3	9.4
Time used# [h]	0.1	2.9	9.6	9.2

#Configuration of PC: 64-bit Windows 7 with IntelXeon E5-1660v3 CPU of 3.0 GHz and memory of 16 GB

Fig. 4 Observation sites at CSUA (upper right diagram) and CSUB (lower right diagram); Tinfoil paper was placed on the north wall near site CSUA to enhance the signal reflection

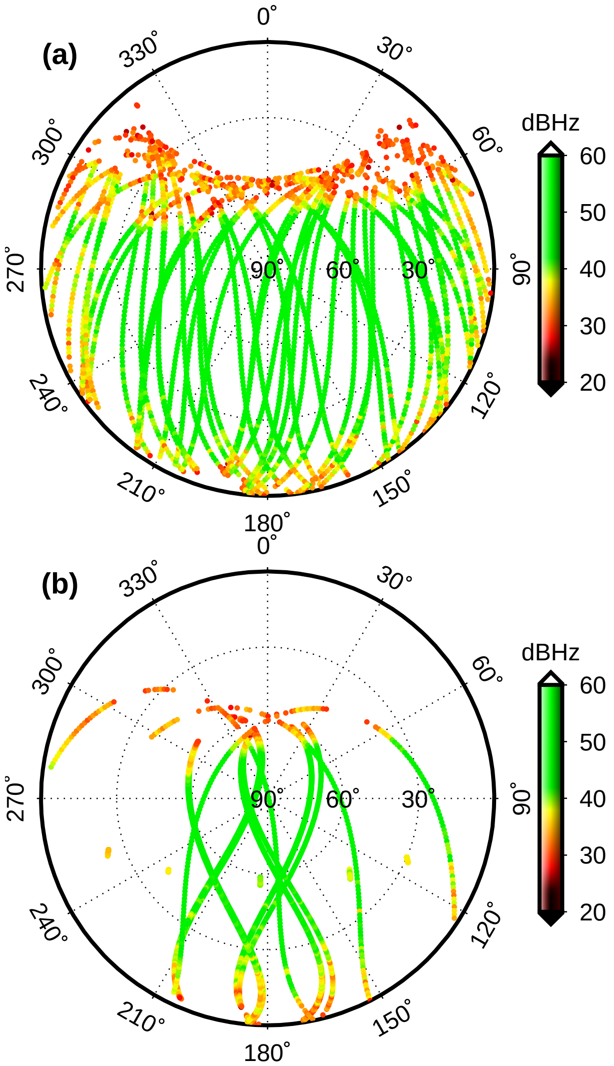

Fig. 5 Sky plots and C/N_0 signal strengths of (a) GPS satellites and (b) Beidou satellites at site CSUA on DOY 320, 2014

Table 3 Solutions of real GNSS dataset from different estimators (3 h×24 sessions)

	LS	VCE	SVE	SVE (VCE)	SVE (GCV)
Repeatability (North component) [mm]	9.6	7.1	5.5	5.5	5.7
Repeatability (East component) [mm]	1.2	0.9	1.4	1.4	1.4
Repeatability (Up component) [mm]	8.9	7.9	6.3	6.4	6.9
Repeatability (Baseline length) [mm]	12.9	10.4	8.3	8.3	8.8
Improvements over LS (Baseline length) [%]	-	19.4	35.6	35.6	31.5
Mean weight-ratio (Beidou/GPS)	1.0	4.1	1.8	1.6	1.0
Mean R-Ratio	12.1	12.1	20.1	20.1	17.4
Mean time used#	2.2 s	2.3 s	0.1 h	2.2 h	10.5 h

#Configuration of PC: 64-bit Windows 7 with IntelXeon E5-1660v3 CPU of 3.0 GHz and memory of 16 GB

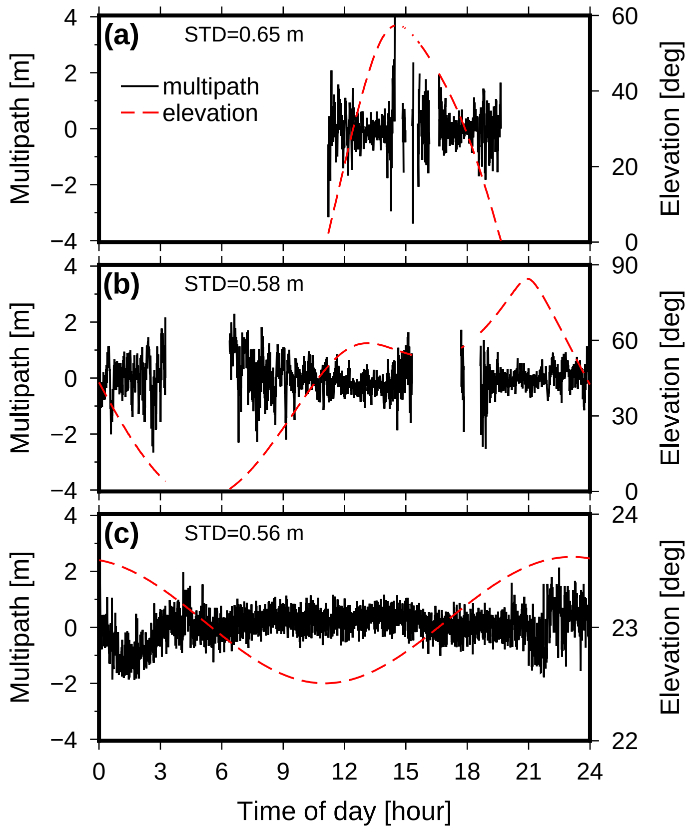

Fig. 6 L1/B1 C/A code multipath v.s. elevations of (a) MEO G31, (b) IGSO C10 and (c) GEO C05 satellites at site CSUA on DOY 320, 2014; The signals of G31 and C10 were blocked by the north wall near the site during the hours of about 14–19

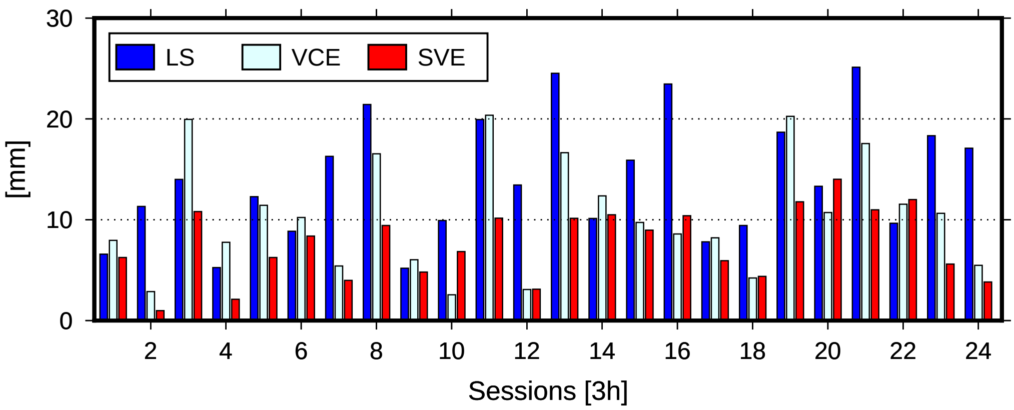

Fig. 7 Baseline length errors of different observation sessions and from different estimators

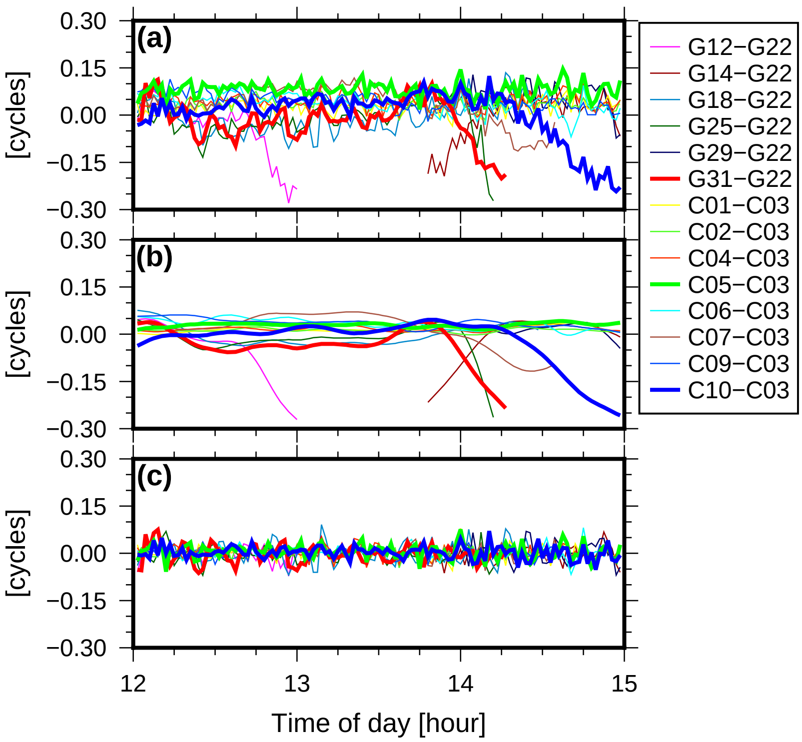

Fig. 8 DD L1/B1 (a) Residuals from LS, (b) Estimated systematic errors from SVE, and (c) Residuals from SVE of the 5-th session

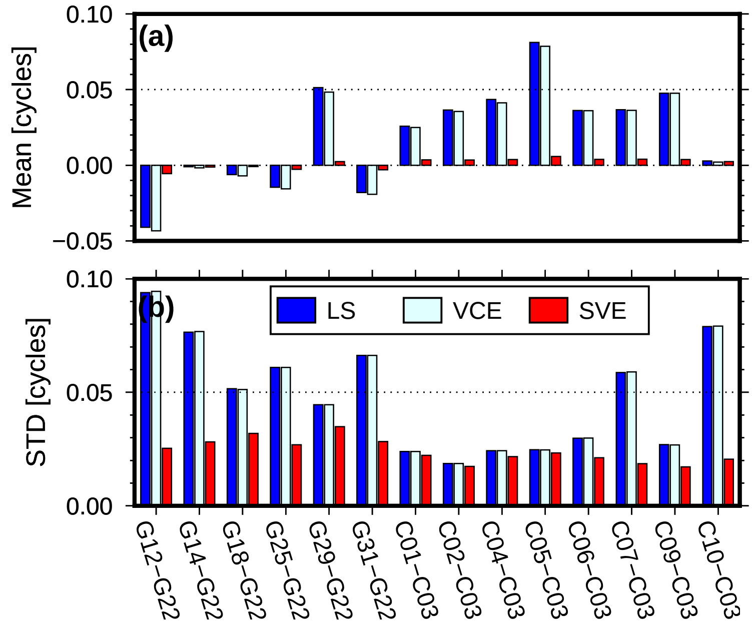

Fig. 9 (a) Means and (b) STDs of DD L1/B1 residuals of the 5-th session

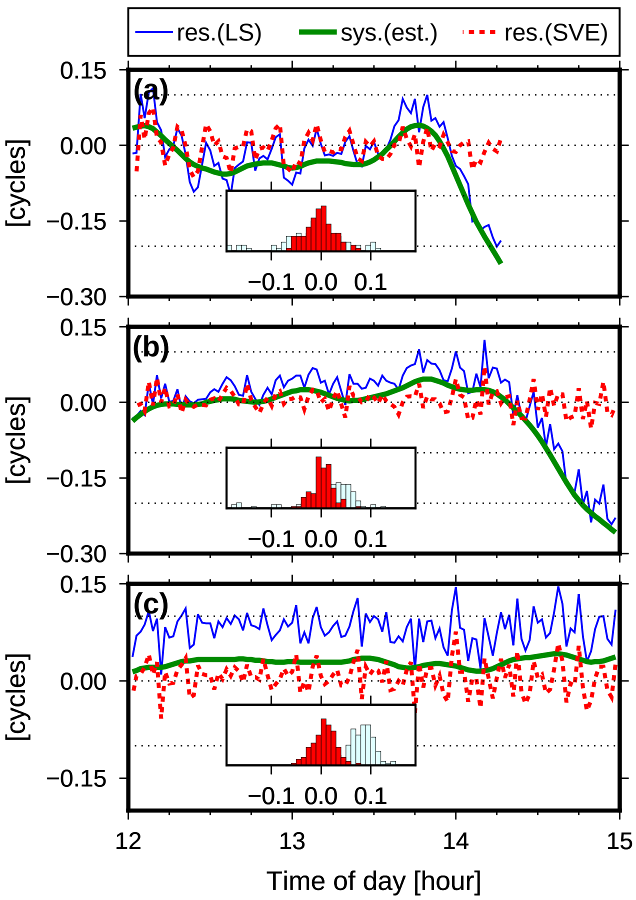

Fig. 10 DD L1/B1 residuals of the 5-th session, satellite pairs (a) G31-G22, (b) C10-C03 and (c) C05-C03 before and after extraction of the systematic errors; Here the 'res.', 'sys.' and 'est.' represent 'residuals', 'systematic errors' and 'estimated', respectively

Table 4 Z-test results of residuals and SPE-derived smoothing parameters (the 5-th session)

Satellite pairs	# of epochs	Z-test (z)		$\hat{\alpha}$ (float solution)	$\hat{\alpha}$
		LS	SVE		
G12-G22	40	6.1	2.5	218.2	215.7
G14-G22	48	6.1	1.0*	373.8	374.2
G18-G22	99	7.2	3.0	215.1	214.7
G25-G22	88	7.9	2.6	179.8	179.3
G29-G22	40	4.9	1.0*	319.2	322.1
G31-G22	91	8.6	4.1	278.1	278.6
C01-C03	119	6.3	-0.3*	10^{15}	437.9
C02-C03	119	8.9	-0.1*	10^{15}	343.8
C04-C03	119	8.9	0.5*	10^{15}	269.7
C05-C03	119	10.1	0.3*	10^{15}	341.2
C06-C03	119	9.0	2.0*	230.5	230.2
C07-C03	103	9.5	1.0*	357.2	357.9
C09-C03	119	9.9	0.4*	397.1	396.7
C10-C03	119	10.1	-0.4*	335.8	335.8

* Residuals that passed the Z-test (significance level 0.01)